Morphological dendritic spine changes of medium spiny neurons in the nucleus accumbens in 6-hydroxydopamine-lesioned rats treated with levodopa

（パーキンソン病モデルラットの側坐核樹状突起神経細胞のスパイン形態変化）

申請者　弘前大学大学院医学研究科

病態制御科学領域　病態病理学教育研究分野

船水　章央

指導教授　水上　浩哉

Abstract

The mechanisms of dopamine dysregulation syndrome (DDS) in Parkinson's disease (PD) remain unclear, although it is known that the nucleus accumbens (NAc) plays a role in its development. Based on the hypothesis that DDS and levodopa-induced dyskinesia (LID) share a pathophysiological basis, we investigated dendritic spine morphology of medium spiny neurons (MSNs) in the NAc of a rat model of LID, because spine enlargement in MSNs of the caudate/putamen has been proposed to be a morphological hallmark of LID. Spines of NAc MSNs also became enlarged in the LID model. This result suggests that excitatory supersensitivity of MSNs in the NAc is involved in the development of DDS, similar to what occurs in the caudate/putamen in LID.

Keywords: dopamine dysregulation syndrome; nucleus accumbens; levodopa-induced dyskinesia; dendritic spine morphology

Abbreviations

DDS, dopamine dysregulation syndrome; PD, Parkinson's disease; NAc, nucleus accumbens; LID, levodopa-induced dyskinesia; CPu, caudate and putamen; MSNs, medium spiny neurons; MFB, medial forebrain bundle; 6-OHDA, 6-hydroxydopamine; AIM, abnormal involuntary movement; LTP, long-term potentiation; LTD, long-term depression

Dopamine dysregulation syndrome (DDS) is an iatrogenic disturbance that may complicate long-term therapy of Parkinson's disease (PD). DDS refers to the addictive patterns of usage of levodopa and, less commonly, apomorphine. The prevalence of DDS in PD patients is estimated to be 3%–4% (Evans and Lees, 2004; Pezzella et al., 2005). A previous study hypothesized that progressive dopaminergic denervation reduces presynaptic dopamine storage mechanisms, which exacerbates the pulsatile effects of levodopa-derived dopamine on limbic structures (Giovannoni et al., 2000). In fact, evidence of maladaptation and sensitization in DDS has been reported as enhanced levodopa-induced dopamine release in the nucleus accumbens (NAc) (Evans et al., 2006), the structure that plays a central role in the development of DDS. However, the molecular mechanisms of DDS remain unclear, largely because there are no validated animal models that replicate the clinical features of DDS (Bastide et al., 2015). Levodopa-induced dyskinesia (LID) and DDS are motor and behavioral complications, respectively, that accompany long-term levodopa treatment. DDS is usually concomitant with LID (Giovannoni et al., 2009; Pezzella et al., 2005). PD patients with LID display enhanced levodopa-derived dopamine release in the caudate and putamen (CPu) (de la Fuente-Fernandez et al., 2004), similar to that which occurs in the NAc of patients with DDS (Evans et al., 2006). These results indicate that dopaminergic overstimulation is a common feature of both LID and DDS in response to levodopa (Giovannoni et al., 2000), suggesting that the CPu in LID and the NAc in DDS share a common molecular abnormality (Linazasoro, 2009; Voon et al., 2009).

Several studies have demonstrated that the dendritic spines of medium spiny neurons (MSNs) in the CPu change their morphology in LID models (Fieblinger et al., 2014; Nishijima et al., 2014; Suarez et al., 2016; Suarez et al., 2014; Zhang et al., 2013).

These morphological changes suggest maladaptive MSN excitatory synapses in the CPu. MSNs are the primary neurons in both the NAc and CPu. Thus, it may be useful to also examine spine morphology of MSNs in the NAc in LID models, to provide a better understanding of the mechanisms involved in DDS. The NAc comprises two functionally and anatomically distinct subregions: the core and the shell (Zahm, 2000; Ito et al., 2004)). In the present study, we evaluated spine morphology of MSN dendritic spines in the NAc core and shell in 6-hydroxydopamine (OHDA)-lesioned PD model rats, repeatedly treated with levodopa, to determine the morphological basis of DDS.

In total, 27 male Wistar rats (CLEA Japan Inc., Tokyo, Japan) were used. The rats were housed in a temperature-controlled room (around 25°C) with a 12-h day/night cycle, with free access to food and water. All efforts were made to minimize the number of animals used and their suffering. This study was approved by the Hirosaki University Animal Experimentation Committee.

At 10 weeks of age, the rats were underwent stereotactic infusion of 6-OHDA or saline into the right medial forebrain bundle (MFB), as previously described (Nishijima et al., 2014), to create unilateral dopaminergic denervation and sham-operation animals, respectively (Fig. 1A). Two weeks after the operation the rats were challenged with apomorphine to evaluate dopaminergic denervation (Maeda et al., 1999) (Fig. 1B).

We treated five 6-OHDA-lesioned hemiparkinsonian rats with saline (PD-Saline group), eight 6-OHDA-lesioned hemiparkinsonian rats with chronic levodopa (PD-Levodopa group), six sham-operated control rats with chronic levodopa (Control-Levodopa group), and eight sham-operated control rats with saline

(Control-Saline group) (Fig. 1B). Beginning 6 weeks after the apomorphine challenge, the 6-OHDA-lesioned and sham-operated rats received 50 mg/kg levodopa methyl ester with 12.5 mg/kg benserazide, a dopa decarboxylase inhibitor (PD-Levodopa group and Control-Levodopa group), or saline (PD-Saline group and Control-Saline group), twice daily for 14 consecutive days (Nishijima et al., 2014) (Fig. 1B). To evaluate the effects of levodopa, we measured abnormal involuntary movement (AIM) scores on days 1, 4, and 11 (Nishijima et al., 2014) (Fig. 1C).

At 20 weeks of age, the rats were anesthetized with sodium pentobarbital (75 mg/kg, intraperitoneally), and intracardially perfused with 4% paraformaldehyde 12 h after the last treatment. Brains were removed and serial 250-μm-thick coronal sections through the NAc were prepared. Sections were dipped in DAPI (4′,6-diamidino-2-phenylindole dihydrochloride) to stain NAc neuronal nuclei. Individual sections were prepared as previously described (Nishijima et al., 2014). MSNs in the NAc core and shell were identified according to diagrams from Paxinos's rat brain atlas (Fig. 2A). Lucifer yellow was injected into MSN cell bodies with DAPI-stained nuclei in the NAc core and shell of the operated hemisphere (Fig. 2A, B, and C) (Nishijima et al., 2014).

Confocal laser scanning microscopy procedures were performed as previously described (Nishijima et al., 2014). We measured spine density and size on the dendrite, 50–100 μm distal to the cell body (Fig. 2C). Image stacks were 3D-deconvoluted using NIS-Elements software (Nikon) and were volume rendered as 3D images to facilitate figure overviews. All spines were 3D reconstructed again, and spine density and volume were quantified, using Neurolucida software (Micro Bright Field, Inc.).

All the drugs except for Nembutal (Dainippon Sumitomo Pharma, Osaka,

Japan) were obtained from Sigma (San Diego, CA, USA).

Quantitative data were evaluated using the Shapiro-Wilk test to determine whether they followed a normal distribution. Spine densities and volumes of spine heads were analyzed using non-parametric tests (Kruskal–Wallis test, followed by the Steel–Dwass multiple comparison test).

All rats that received levodopa treatment after 6-OHDA lesioning (PD-Levodopa group) displayed AIMs during the treatment period (Fig. 1C). The total AIM score in the PD-Levodopa group on day 11 was more than twice the score on day 1. However, control rats that received levodopa treatment (Control-Levodopa group) did not show AIMs (Fig. 1C). The PD-Levodopa group was regarded as a validated LID model (Cenci et al., 1998).

Dopaminergic denervation significantly decreased MSN spine density in the NAc core (Control-Saline: 8.6 ± 2.3/μm; PD-Saline: 4.9 ± 0.5/μm) and shell (Control-Saline: 8.5 ± 2.5/μm; PD-Saline: 5.0 ± 0.2/μm) compared with controls (Fig. 2D, E). Repeated levodopa treatment restored the dopamine-denervation-induced decrease in spine density in both the core (PD-Levodopa: 7.8 ± 1.0/μm) and shell (PD-Levodopa: 8.4 ± 1.4/μm) (Fig. 2D, E). In the Control-Saline group, levodopa treatment had no effect on spine density (Fig. 2D, E). Spine volume in the NAc did not change after dopaminergic denervation (Fig. 2D, F, PD-Saline group). However, chronic levodopa treatment significantly increased the average volume of MSN dendritic spines in both the core (PD-Saline: 0.12 ± 0.02 μm^3; PD-Levodopa : 0.27 ± 0.07 μm^3) and shell (PD-Saline: 0.13 ± 0.04 μm^3; PD-Levodopa: 0.21 ± 0.03 μm^3) in animals with dopaminergic denervation (PD-Levodopa group) compared with those in the PD-Saline group (Fig.

2D, F). In the normal NAc, levodopa treatment increased spine volume in the shell (Control-Saline: 0.15 ± 0.04 μm^3; Control-Levodopa: 0.22 ± 0.06 μm^3), but not in the core (Control-Saline: 0.15 ± 0.03 μm^3; Control-Levodopa: 0.16 ± 0.07 μm^3) (Fig. 2F).

We found that dopamine denervation decreased spine density of MSNs in both the core and shell of the NAc, and levodopa treatment restored this spine density. Dopamine denervation in normal rats had no effect on spine volume of NAc MSNs, but levodopa treatment in the PD model increased spine volume with a concomitant development of dyskinesia.

The decrease of spine density in the NAc of 6-OHDA-lesioned rats (Fig. 2E) was consistent with previous results (Meredith et al., 1995; Solis et al., 2007). A loss of spines is also found in MSNs of the CPu in PD patients and PD models (Nishijima et al., 2014; Stephens et al., 2005; Suarez et al., 2014; Villalba and Smith, 2010). The mechanisms of this spine loss remain unknown (Villalba and Smith, 2010). Levodopa treatment restored the dopamine-denervation-induced decrease in spine density in the NAc (Fig. 2D, E). This recovery has also been reported in the CPu of PD models (Suarez et al., 2014; Zhang et al., 2013). However, restoration of MSN spine density was accompanied by an enlargement of the spines in both the core and shell (Fig. 2D, F). This enlargement has also been observed in MSNs of the CPu in the same LID model (Nishijima et al., 2014). The large and small spines correlate with forms of synaptic plasticity, such as long-term potentiation (LTP) and long-term depression (LTD), respectively (Holtmaat and Svoboda, 2009; Kasai et al., 2010). At a molecular level, it is believed that LTP and LTD alter actin polymerization, which affects spine maturation and stability, and also either anchor or internalize α-amino-3-hydroxyl-5-methyl-4-isoxazole-propionate (AMPA) receptors to produce

more functional spines (LTP) or retraction of existing spines (LTD) (Matsuzaki et al., 2004; Tada and Sheng, 2006). Upon stabilization, spines become large and mushroom-shaped, have larger postsynaptic densities, show increased surface expression of AMPA receptors, and persist for months (Holtmaat and Svoboda, 2009). Spine enlargement in NAc neurons has been shown to be strictly regulated by glutamatergic and dopaminergic afferents (Yagishita et al., 2014). The enlargement reflects a highly stable cellular event, which could explain why certain long-term behavioral changes are associated with addiction and/or levodopa-induced dyskinesia (Nishijima et al., 2014; Russo et al., 2010). Thus, spines of MSNs in the NAc of the LID model seem to become supersensitive to excitatory inputs, similar to those of MSNs in the CPu (Nishijima et al., 2014). In the CPu, the direct pathway neurons that bear dopamine D1 receptors, but not the indirect pathway neurons that bear D2 receptors, displayed spine enlargement (Nishijima et al., 2014). MSNs in the NAc also consist of two types of neurons: those that express D1 receptors, and those that express D2 receptors. However, functional and anatomical differences between the two neuron types in the NAc are much less understood when compared with those of CPu MSNs. Differences in morphological changes between the two neuron types in the NAc should be investigated in any future studies.

It is of note that Control-Levodopa rats also exhibited enlargement of MSN spines in the NAc shell, but not in the core (Fig. 2D, F), without any behavioral changes (Fig. 1C). A previous study reported that high-dose levodopa treatment in normal rats slightly increased extracellular dopamine levels in the CPu (Maeda et al., 1999). Accordingly, structural changes can occur in MSN dendritic spines in the normal NAc. Because spine enlargement in the shell was also observed in the Control-Levodopa

group (Fig. 2F), the significance of spine enlargement in the shell for the behavioral changes is ambiguous. Previous studies have shown that the shell is preferentially involved in the development of drug addiction, whereas the core mediates long-term execution of learned addiction-related behaviors (Ito et al., 2004; Meredith et al., 2008). Namely, enlargement of shell spines may reveal the initial onset of levodopa-induced behaviors, whereas that of core spines may represent enduring levodopa-induced abnormal behaviors. This could result from the fact that glutamate-dopamine convergence is higher in the core than in the shell (Zahm and Brog, 1992).

In the LID model, enlargement of MSN dendritic spines in the CPu is a pathological hallmark (Nishijima et al., 2014; Suarez et al., 2016). Enlargement of MSN spines in the NAc, especially in the core, may therefore be the most important pathological finding. The levodopa-seeking behavior in patients with DDS is similar to the behavioral dependence observed in drug addiction (Evans et al., 2010; Linazasoro, 2009). Growing evidence shows that morphological changes in MSN spines in the NAc are related to addictive behavior in cocaine use (Shen et al., 2009), which increases synaptic dopamine levels (Weiss et al., 1992). MSN spines in the NAc become enlarged in the withdrawal phase of cocaine exposure (Russo et al., 2010). Thus, enlargement of MSN spines in the NAc may account for the psychological dependence of cocaine addiction (Russo et al., 2010). Taken together, MSN spine enlargement in the NAc may represent a pathological hallmark associated with behavioral dependence on levodopa in DDS. However, we investigated MSN spines of the LID model, and not of a DDS model. This problem is a limitation that must be acknowledged when considering the present results. It is thus warranted to create a distinct model of DDS to address this limitation.

Figure Legends

Fig. 1 (A). Tyrosine hydroxylase immunohistochemistry from a section through the nucleus accumbens of a 6-hydroxydopamine-lesioned rat. The lesioned side of the striatum, not stained by tyrosine hydroxylase, is indicated by an asterisk (*). (**B)**. Time chart and experimental design. We injected 6-hydroxydopamine (6-OHDA) or saline into the medial forebrain bundle at 10 weeks of age to establish a hemiparkinsonian model (PD-Levodopa group; PD-Saline group) or sham-operated model (Control-Saline group; Control-Levodopa group), respectively. At 12 weeks of age, 6-OHDA-treated rats were challenged with an apomorphine injection to confirm dopaminergic denervation. The PD-Levodopa group and Control-Levodopa group received daily levodopa treatment, and the PD-Saline group and Control-Saline group received daily saline injections, from 18 weeks. At 20 weeks, all rats were sacrificed and processed for pathological examinations. (**C)**, Changes in abnormal involuntary movement (AIM) scores of control rats treated with levodopa (Control-Levodopa group) or unilaterally 6-OHDA-lesioned rats treated with levodopa (PD-Levodopa group) on days 1, 4, and 11. Control-Levodopa group rats showed no AIM, whereas rats in the PD-Levodopa group showed progressive deterioration of dyskinesias following the commencement of levodopa treatment. (Kruskal–Wallis test followed by Steel–Dwass multiple comparison test: ** $P < 0.001$ vs. day 1, $^{\#\#} P < 0.001$ vs. day 4). Control-Levodopa group rats showed no AIMs..

Fig. 2 (A), Image of microinjected medium spiny neurons in the core and shell of the nucleus accumbens (NAc). ACA; anterior part of the anterior commissure. Scale bar = 100 μm.

(**B)**, Representative confocal laser-scanning image of a medium spiny neuron in the core of the nucleus accumbens as visualized by Lucifer yellow. Scale bar = 20 μm. **(C)** Density and volume of spines were measured on dendrites located 50–100 μm from the cell body (higher magnification of the image from the white box in B). Scale bar = 5 μm.

Fig. 2D–F, Morphological evaluation of dendritic spines. (**D)**, Representative confocal microscope images of dendritic spines of medium spiny neurons in the core and shell of the nucleus accumbens from 250-μm-thick tissue preparations from Control-Saline, PD-Saline, PD-Levodopa, and Control-Levodopa groups. Scale bar = 5 μm. Quantitative evaluations of density (**E**) and volume (**F**) of dendritic spines of medium spiny neurons in the core and shell. (**E)**, Spine density is significantly decreased in the PD-Saline group. Levodopa treatment restores spine density. (Core. Control-Saline: 8.6 ± 2.3/μm; PD-Saline: 4.9 ± 0.5/μm; PD-Levodopa: 7.8 ± 1.0/μm; Control-Levodopa: 8.2 ± 1.5/μm. Shell. Control-Saline: 8.5 ± 2.5/μm; PD-Saline: 5.0 ± 0.2/μm; PD-Levodopa: 8.4 ± 1.4/μm; Control-Levodopa: 7.4 ± 2.0/μm). (**F)**, Levodopa treatment increases spine volume of medium spiny neurons in the core and shell in the PD-Levodopa group. Enlargement of spines is seen only in the shell of the Control-Levodopa group. (Core. Control-Saline: 0.15 ± 0.03 μm^3; PD-Saline: 0.12 ± 0.02 μm^3; PD-Levodopa: 0.27 ± 0.07 μm^3; Control-Levodopa: 0.16 ± 0.07 μm^3. Shell. Control-Saline: 0.15 ± 0.04 μm^3; PD-Saline: 0.13 ± 0.04 μm^3; PD-Levodopa: 0.21 ± 0.03 μm^3; Control-Levodopa: 0.22 ± 0.06 μm^3). (*$P < 0.05$, **$P < 0.01$, Kruskal–Wallis test followed by the Steel–Dwass multiple comparison test).

Author contributions

Conceived and designed the experiments: Y.F. and M.T. Performed the experiments: Y.F. and M.T. Analyzed the data: Y.F. and T.U. Wrote the paper: Y.F. and H.N. and M.T. Critical revision of the article for important intellectual content: S.Y. and H.M.

Conflict of interest

The authors have no conflict of interest directly relevant to the content of this article.

Acknowledgments

The authors thank Prof. Hiroshi Shimoda for his kind support in our study.

References

Bastide, M.F., Meissner, W.G., Picconi, B., Fasano, S., Fernagut, P.O., Feyder, M., Francardo, V., Alcacer, C., Ding, Y., Brambilla, R., Fisone, G., Jon Stoessl, A., Bourdenx, M., Engeln, M., Navailles, S., De Deurwaerdere, P., Ko, W.K., Simola, N., Morelli, M., Groc, L., Rodriguez, M.C., Gurevich, E.V., Quik, M., Morari, M., Mellone, M., Gardoni, F., Tronci, E., Guehl, D., Tison, F., Crossman, A.R., Kang, U.J., Steece-Collier, K., Fox, S., Carta, M., Angela Cenci, M., Bezard, E., 2015. Pathophysiology of L-dopa-induced motor and non-motor complications in Parkinson's disease. Progress in neurobiology 132, 96-168.

de la Fuente-Fernandez, R., Sossi, V., Huang, Z., Furtado, S., Lu, J.Q., Calne, D.B., Ruth, T.J., Stoessl, A.J., 2004. Levodopa-induced changes in synaptic dopamine levels increase with progression of Parkinson's disease: implications for dyskinesias. Brain : a journal of neurology 127, 2747-2754.
Di Chiara, G., 2002. Nucleus accumbens shell and core dopamine: differential role in behavior and addiction. Behavioural brain research 137, 75-114.

Evans, A.H., Lees, A.J., 2004. Dopamine dysregulation syndrome in Parkinson's disease. Current opinion in neurology 17, 393-398.

Evans, A.H., Pavese, N., Lawrence, A.D., Tai, Y.F., Appel, S., Doder, M., Brooks, D.J., Lees, A.J., Piccini, P., 2006. Compulsive drug use linked to sensitized ventral striatal dopamine transmission. Annals of neurology 59, 852-858.

Fieblinger, T., Graves, S.M., Sebel, L.E., Alcacer, C., Plotkin, J.L., Gertler, T.S., Chan, C.S., Heiman, M., Greengard, P., Cenci, M.A., Surmeier, D.J., 2014. Cell type-specific plasticity of striatal projection neurons in parkinsonism and L-DOPA-induced dyskinesia. Nature communications 5, 5316.

Giovannoni, G., O'Sullivan, J.D., Turner, K., Manson, A.J., Lees, A.J., 2000. Hedonistic homeostatic dysregulation in patients with Parkinson's disease on dopamine replacement therapies. Journal of neurology, neurosurgery, and psychiatry 68, 423-428.

Holtmaat, A., Svoboda, K., 2009. Experience-dependent structural synaptic plasticity in the mammalian brain. Nature reviews. Neuroscience 10, 647-658.

Ito, R., Robbins, T.W., Everitt, B.J., 2004. Differential control over cocaine-seeking behavior by nucleus accumbens core and shell. Nature

neuroscience 7, 389-397.

Kasai, H., Fukuda, M., Watanabe, S., Hayashi-Takagi, A., Noguchi, J., 2010. Structural dynamics of dendritic spines in memory and cognition. Trends in neurosciences 33, 121-129.

Linazasoro, G., 2009. Dopamine dysregulation syndrome and levodopa-induced dyskinesias in Parkinson disease: common consequences of anomalous forms of neural plasticity. Clinical neuropharmacology 32, 22-27.
Maeda, T., Kannari, K., Suda, T., Matsunaga, M., 1999. Loss of regulation by presynaptic dopamine D2 receptors of exogenous L-DOPA-derived dopamine release in the dopaminergic denervated striatum. Brain research 817, 185-191.

Maeda, T., Kannari, K., Suda, T., Matsunaga, M., 1999. Loss of regulation by presynaptic dopamine D2 receptors of exogenous L-DOPA-derived dopamine release in the dopaminergic denervated striatum. Brain research 817, 185-191.

Matsuzaki, M., Honkura, N., Ellis-Davies, G.C., Kasai, H., 2004. Structural basis of long-term potentiation in single dendritic spines. Nature 429, 761-766.

Meredith, G.E., Baldo, B.A., Andrezjewski, M.E., Kelley, A.E., 2008. The structural basis for mapping behavior onto the ventral striatum and its subdivisions. Brain structure & function 213, 17-27.

Meredith, G.E., Ypma, P., Zahm, D.S., 1995. Effects of dopamine depletion on the morphology of medium spiny neurons in the shell and core of the rat nucleus accumbens. The Journal of neuroscience : the official journal of the Society for Neuroscience 15, 3808-3820.

Nishijima, H., Suzuki, S., Kon, T., Funamizu, Y., Ueno, T., Haga, R., Suzuki, C., Arai, A., Kimura, T., Suzuki, C., Meguro, R., Miki, Y., Yamada, J., Migita, K., Ichinohe, N., Ueno, S., Baba, M., Tomiyama, M., 2014. Morphologic changes of dendritic spines of striatal neurons in the levodopa-induced dyskinesia model. Movement disorders : official journal of the Movement Disorder Society 29, 336-343.

Pezzella, F.R., Colosimo, C., Vanacore, N., Di Rezze, S., Chianese, M., Fabbrini, G., Meco, G., 2005. Prevalence and clinical features of hedonistic homeostatic dysregulation in Parkinson's disease. Movement disorders : official journal of the Movement Disorder Society 20, 77-81.

Russo, S.J., Dietz, D.M., Dumitriu, D., Morrison, J.H., Malenka, R.C.,

Nestler, E.J., 2010. The addicted synapse: mechanisms of synaptic and structural plasticity in nucleus accumbens. Trends in neurosciences 33, 267-276.

Shen, H.W., Toda, S., Moussawi, K., Bouknight, A., Zahm, D.S., Kalivas, P.W., 2009. Altered dendritic spine plasticity in cocaine-withdrawn rats. The Journal of neuroscience : the official journal of the Society for Neuroscience 29, 2876-2884.

Solis, O., Limon, D.I., Flores-Hernandez, J., Flores, G., 2007. Alterations in dendritic morphology of the prefrontal cortical and striatum neurons in the unilateral 6-OHDA-rat model of Parkinson's disease. Synapse 61, 450-458.

Stephens, B., Mueller, A.J., Shering, A.F., Hood, S.H., Taggart, P., Arbuthnott, G.W., Bell, J.E., Kilford, L., Kingsbury, A.E., Daniel, S.E., Ingham, C.A., 2005. Evidence of a breakdown of corticostriatal connections in Parkinson's disease. Neuroscience 132, 741-754.

Suarez, L.M., Solis, O., Aguado, C., Lujan, R., Moratalla, R., 2016. L-DOPA Oppositely Regulates Synaptic Strength and Spine Morphology in D1 and D2 Striatal Projection Neurons in Dyskinesia. Cerebral cortex (New York, N.Y. : 1991).

Suarez, L.M., Solis, O., Carames, J.M., Taravini, I.R., Solis, J.M., Murer, M.G., Moratalla, R., 2014. L-DOPA treatment selectively restores spine density in dopamine receptor D2Fxpressing projection neurons in dyskinetic mice. Biological psychiatry 75, 711-722.

Tada, T., Sheng, M., 2006. Molecular mechanisms of dendritic spine morphogenesis. Current opinion in neurobiology 16, 95-101.

Villalba, R.M., Smith, Y., 2010. Striatal spine plasticity in Parkinson's disease. Frontiers in neuroanatomy 4, 133.

Voon, V., Fernagut, P.O., Wickens, J., Baunez, C., Rodriguez, M., Pavon, N., Juncos, J.L., Obeso, J.A., Bezard, E., 2009. Chronic dopaminergic stimulation in Parkinson's disease: from dyskinesias to impulse control disorders. The Lancet. Neurology 8, 1140-1149.

Weiss, F., Paulus, M.P., Lorang, M.T., Koob, G.F., 1992. Increases in extracellular dopamine in the nucleus accumbens by cocaine are inversely related to basal levels: effects of acute and repeated administration. The Journal of neuroscience : the official journal of the Society for Neuroscience 12, 4372-4380.

Yagishita, S., Hayashi-Takagi, A., Ellis-Davies, G.C., Urakubo, H., Ishii, S., Kasai, H., 2014. A critical time window for dopamine actions on the structural plasticity of dendritic spines. Science (New York, N.Y.) 345, 1616-1620.

Zahm, D.S., 2000. An integrative neuroanatomical perspective on some subcortical substrates of adaptive responding with emphasis on the nucleus accumbens. Neuroscience and biobehavioral reviews 24, 85-105.

Zahm, D.S., Brog, J.S., 1992. On the significance of subterritories in the "accumbens" part of the rat ventral striatum. Neuroscience 50, 751-767.

Zhang, Y., Meredith, G.E., Mendoza-Elias, N., Rademacher, D.J., Tseng, K.Y., Steece-Collier, K., 2013. Aberrant restoration of spines and their synapses in L-DOPA-induced dyskinesia: involvement of corticostriatal but not thalamostriatal synapses. The Journal of neuroscience : the official journal of the Society for Neuroscience 33, 11655-11667.

A

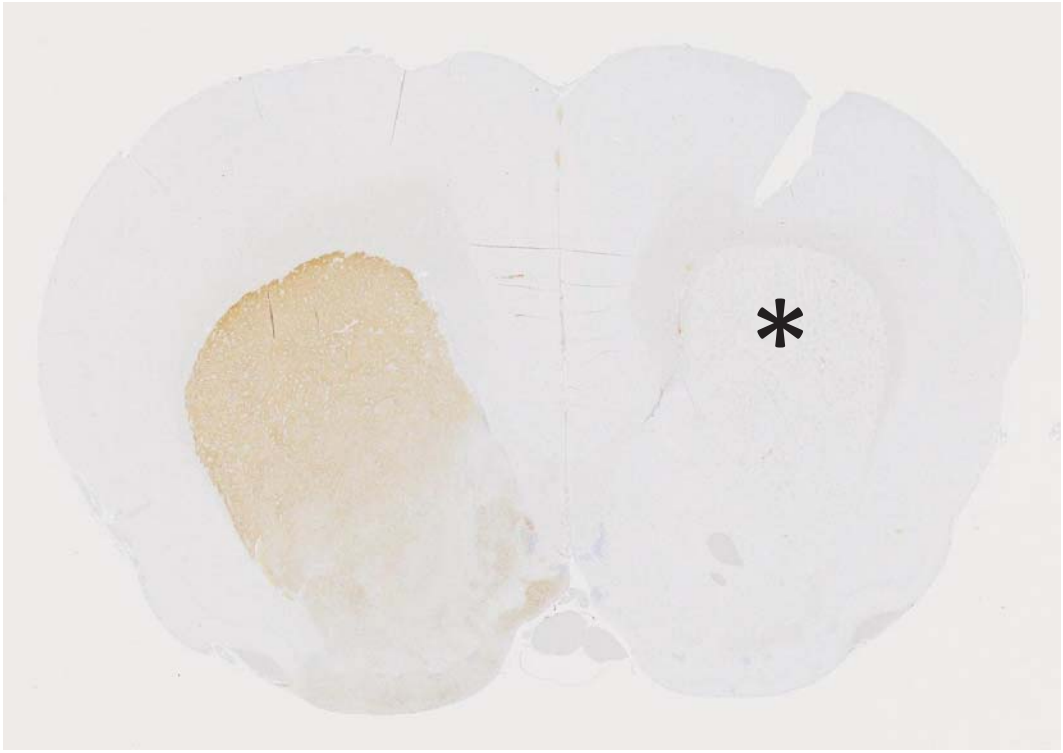
*

B

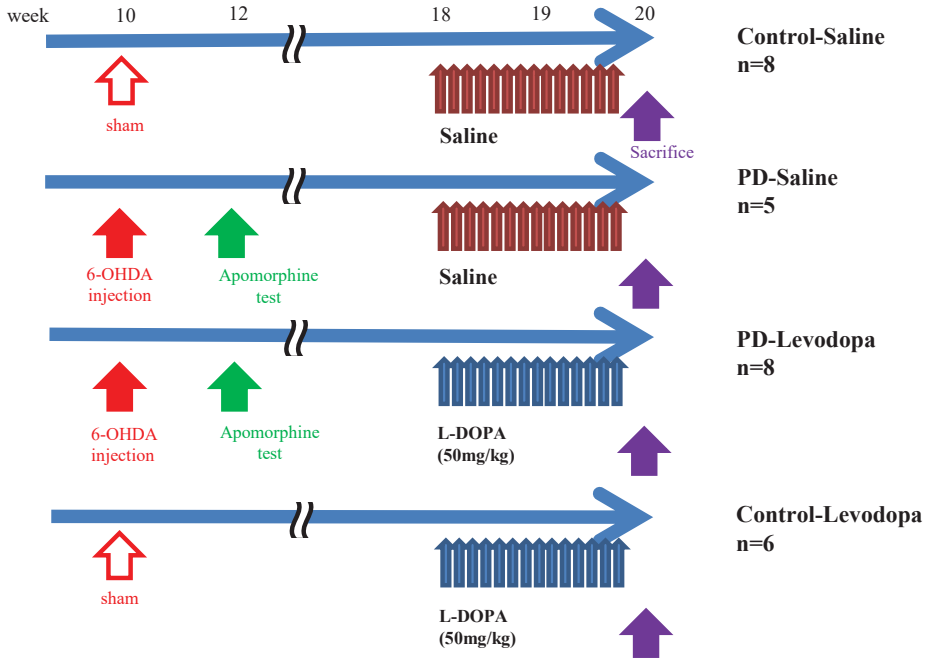
week
10
12
18
19
20
sham
Saline
Sacrifice
Control-Saline
n=8
6-OHDA injection
Apomorphine test
Saline
PD-Saline
n=5
6-OHDA injection
Apomorphine test
L-DOPA (50mg/kg)
PD-Levodopa
n=8
sham
L-DOPA (50mg/kg)
Control-Levodopa
n=6

C

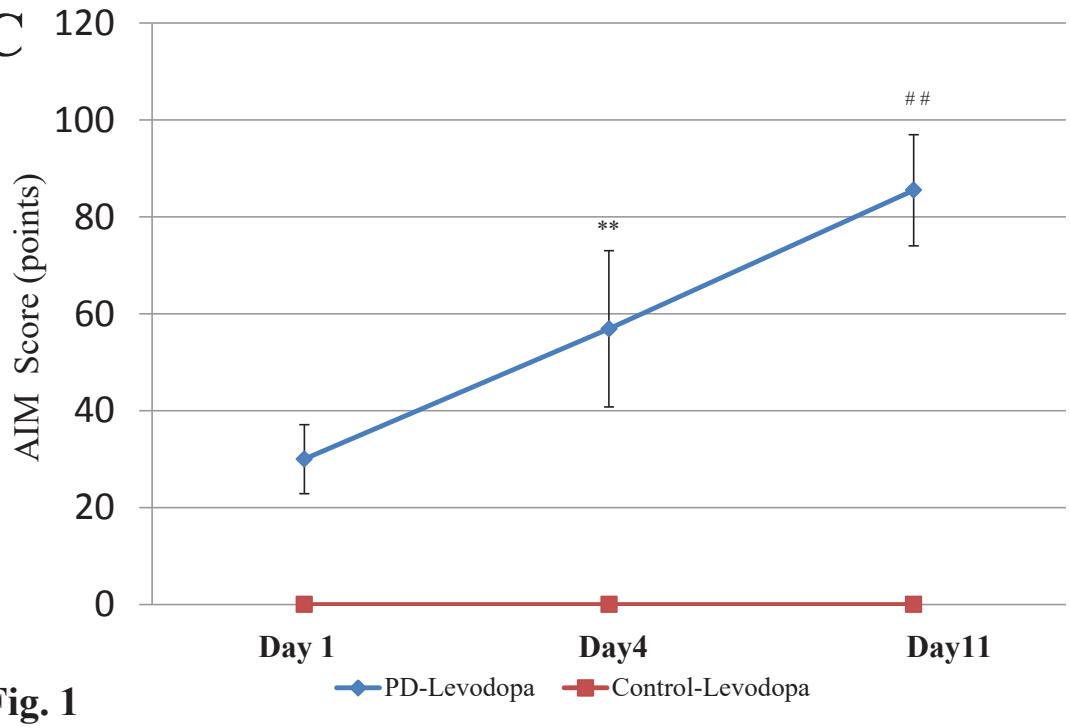
AIM Score (points)
120
100
80
60
40
20
0
**
##
Day 1
Day4
Day11
PD-Levodopa
Control-Levodopa

Fig. 1

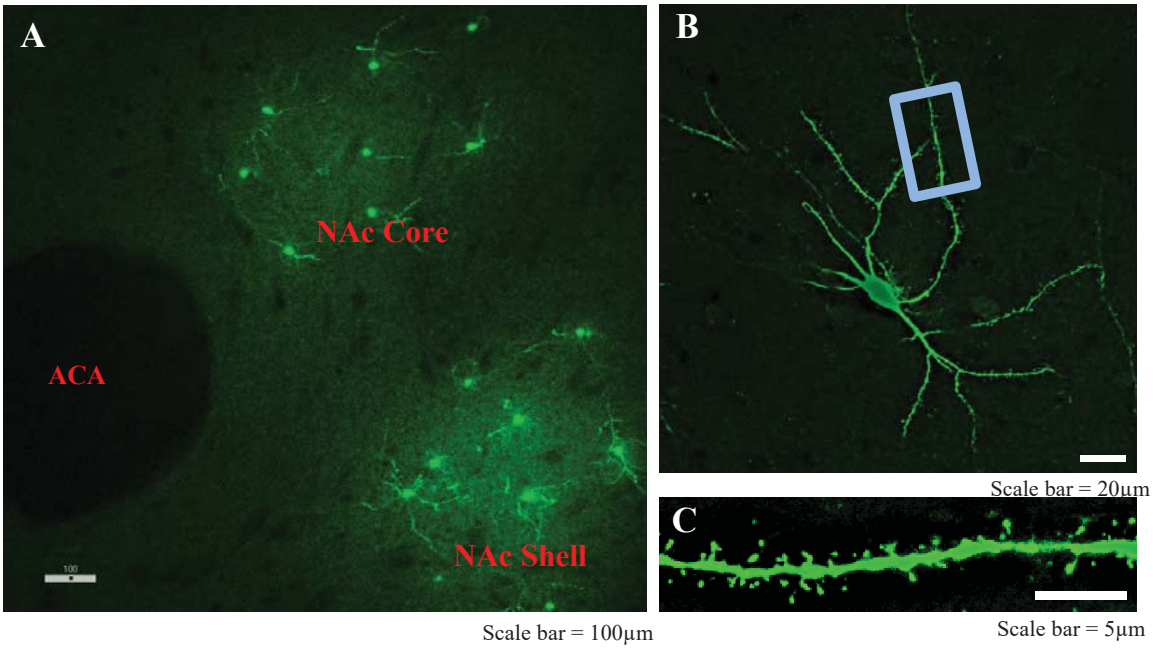
A
NAc Core
ACA
NAc Shell
Scale bar = 100µm
B
Scale bar = 20µm
C
Scale bar = 5µm

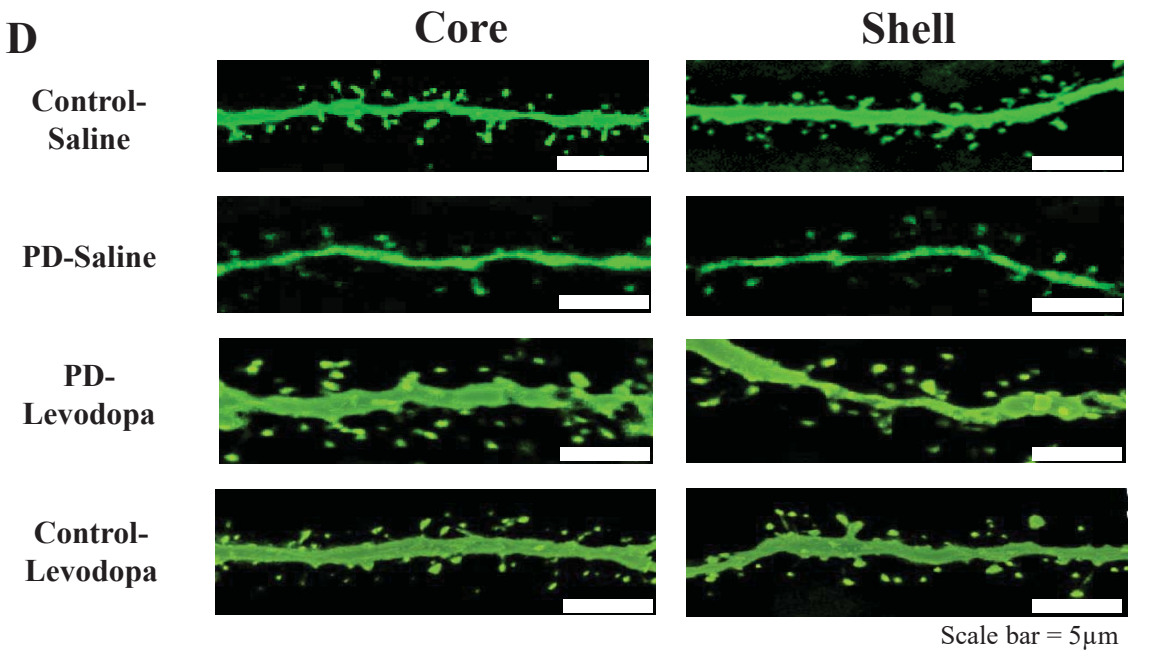
D
Core
Shell
Control-Saline
PD-Saline
PD-Levodopa
Control-Levodopa
Scale bar = 5µm

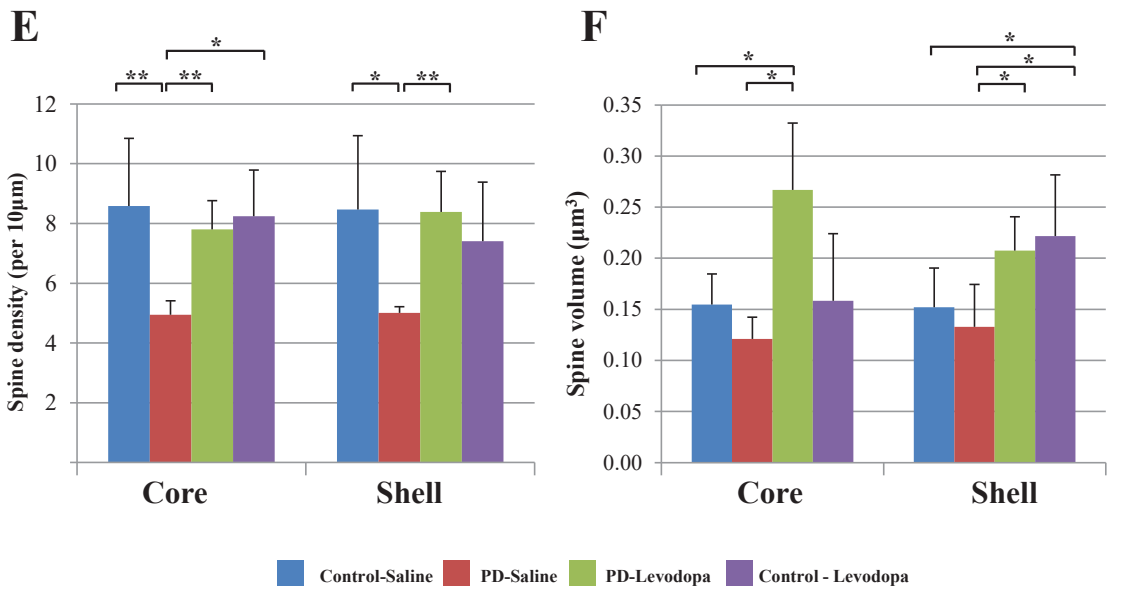
E
F
Spine density (per 10µm)
Spine volume (µm³)
Core
Shell
Control-Saline
PD-Saline
PD-Levodopa
Control - Levodopa

Fig. 2